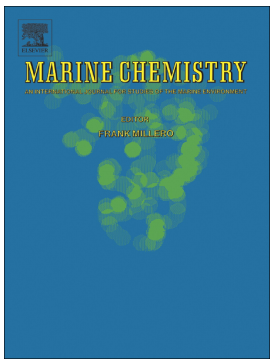

The great barrier reef: A source of CO2 to the atmosphere

Christian Lønborg, Maria Ll Calleja, Katharina E. Fabricius, Joy N. Smith, Eric P. Achterberg

PII: S0304-4203(18)30047-1
DOI: https://doi.org/10.1016/j.marchem.2019.02.003
Reference: MARCHE 3633

To appear in: *Marine Chemistry*

Received date: 22 February 2018
Revised date: 21 January 2019
Accepted date: 8 February 2019

Please cite this article as: C. Lønborg, M.L. Calleja, K.E. Fabricius, et al., The great barrier reef: A source of CO2 to the atmosphere, Marine Chemistry, https://doi.org/10.1016/j.marchem.2019.02.003

The Great Barrier Reef: A source of CO_2 to the atmosphere

Christian Lønborg[1*], Maria Ll. Calleja[2], Katharina E. Fabricius[1], Joy N. Smith[1], & Eric P. Achterberg[3]

[1]Australian Institute of Marine Science, PMB No 3, Townsville, Queensland 4810, Australia

[2]King Abdullah University of Science and Technology (KAUST), Division of Biological and Environmental Sciences and Engineering (BESE), Red Sea Research Center (RSRC), Thuwal, 23955-6900, Saudi Arabia

[3]GEOMAR Helmholtz Centre for Ocean Research, 24148 Kiel, Germany

[*]Corresponding author:

Australian Institute of Marine Science

PMB 3, Townsville MC, QLD 4810

Australia

Phone: 0061 (0) 7 4753 4382

Fax: 0061 (0) 7 4772 5852

Email: clonborg@gmail.com

Abstract

The Great Barrier Reef (GBR) is the largest contiguous coral reef system in the world. Carbonate chemistry studies and flux quantification within the GBR have largely focused on reef calcification and dissolution, with relatively little work on shelf-scale CO_2 dynamics. In this manuscript, we describe the shelf-scale seasonal variability in inorganic carbon and air-sea CO_2 fluxes over the main seasons (wet summer, early dry and late dry seasons) in the GBR.

Our large-scale dataset reveals that despite spatial-temporal variations, the GBR as a whole is a net source of CO_2 to the atmosphere, with calculated air–sea fluxes varying between -6.19 and 12.17 mmol m^{-2} d^{-1} (average ± standard error: 1.44 ± 0.15 mmol m^{-2} d^{-1}), with the strongest release of CO_2 occurring during the wet season. The release of CO_2 to the atmosphere is likely controlled by mixing of Coral Sea surface water, typically oversaturated in CO_2, with the warm shelf waters of the GBR. This leads to oversaturation of the GBR system relative to the atmosphere and a consequent net CO_2 release.

Keywords: Air-sea CO_2 flux; marine inorganic carbon chemistry; seawater carbonate chemistry; Great Barrier Reef

Introduction

The marine carbon cycle has undergone dramatic changes since the Industrial Revolution mainly due to the anthropogenic emissions to the atmosphere of carbon dioxide (CO_2), of which the ocean has taken up around 30 % (Le Quéré et al., 2016). This uptake is altering the marine carbonate system and reducing seawater pH (Doney et al., 2009), with the extent of acidification influenced by complex interactions between physical, chemical, biological, and geological processes.

Carbon cycling is intense in coastal waters, with approximately 815 Tmol C yr^{-1} of primary production, inputs of around 80 Tmol C yr^{-1} (inorganic and organic) from terrestrial sources, and storage of around 40 Tmol C yr^{-1} in sediments (Andersson et al., 2005; Jahnke, 2010). Global estimates suggest that, overall, coastal waters are sinks for atmospheric CO_2, with a total uptake of around 20 Tmol C yr^{-1}, but that the magnitude of this sink varies both spatially and temporally (Chen and Borges, 2009). From a spatial perspective it is important to distinguish between offshore (generally CO_2 sink) and near-shore coastal waters (mainly CO_2 source), and high and temperate latitudes (CO_2 sink) versus subtropical and tropical waters (CO_2 source) (Cai et al., 2006; Chen and Borges, 2009). These spatial heterogeneities in the sources and sinks are partially driven by differences in seawater temperatures, carbon supply by rivers, and community metabolism (primary production and respiration) (Chen et al., 2013). The solubility of CO_2 in seawater is strongly temperature dependent with a rise in temperatures increasing the surface ocean CO_2 partial pressure (pCO_2) and reducing the CO_2 sink capacity of the system. At the temperature threshold when the sea surface becomes oversaturated with pCO_2, the air-sea gradient reverses and the system becomes a CO_2 source to the atmosphere (Takahashi et al., 1993; Weiss, 1974). Spatial and seasonal differences in the magnitude of terrestrial inputs (i.e. nutrients, organic matter), and the subsequent biogeochemical processes, including community metabolism , also affect surface water pCO_2 and determine if a system acts as a net source or sink of CO_2 to the atmosphere (Borges and Abril, 2012; Cai et al., 2006; Cai, 2011; Chen et al., 2013). Thereby, seasonal changes in wind, weather patterns,

temperature, river inputs, as well as community primary production and respiration can impact the CO_2 uptake/release and export (Thomas et al., 2004; Tsunogai et al., 1999).

Only around 11% of the global shelf waters lie within the tropics (Jahnke, 2010). Nevertheless they receive more continental derived carbon, nitrogen and phosphorus than temperate and Arctic regions (Brunskill, 2010). Seawater in tropical coral reefs is generally oligotrophic, but tropical coastal waters influenced by river discharge are characterized by relatively high productivity which is also sustained by elevated temperatures and high sunlight levels, with phytoplankton production rates, in some instances, matching some of the most productive areas of the global ocean (e.g. upwelling regions) (Nittrouer et al., 1995). Tropical coastal waters are also hosts to most of the global benthic oceanic calcium carbonate ($CaCO_3$) producers (e.g. corals, coralline algae, foraminifera) and account for around 40% of the global oceanic $CaCO_3$ production and accumulation (Balch, 2005; Gattuso et al., 1998; Milliman, 1993). The impact of $CaCO_3$ production and dissolution is especially important on carbon fluxes in tropical coastal waters, such as the Great Barrier Reef (GBR), which hosts scleractinian corals. For example, during the production of 1 mol of $CaCO_3$, 0.6 mol of CO_2 are released to the surrounding waters (Ware et al., 1991). Although tropical coastal systems are important for the global cycling and storage of carbon, relatively few studies have investigated the variability of or determined the factors that influence the marine carbonate system and air-sea CO_2 fluxes in these regions (Kinsey and Hopley, 1991; Smith and Key, 1975; Smith and Pesret, 1974; Suzuki and Kawahata, 1999).

The GBR is situated on the NE Australia continental shelf between 9 and 24°S and is the largest contiguous coral reef system in the world. Previous studies on carbonate chemistry and carbon fluxes within the GBR system have largely focused on reef calcification and dissolution, whereas comparatively little work has been done on the shelf-scale dynamics of inorganic carbon and the air-sea fluxes of CO_2 (Cyronak et al., 2014; Kawahata et al., 2000; Lenton et al., 2016; Mongin et al., 2016; Suzuki and Kawahata, 2003; Uthicke et al., 2014). The aim of this study was to determine the

temporal-spatial patterns in the air-sea flux of CO_2 and to establish if the GBR is overall a net source or sink of CO_2.

Materials and Methods

Study area - The GBR has a maximum width of 330 km and extends over an area of 344,000 km^2 (Figure 1). Coral reefs and seagrasses occupy around 7% and 20% of shelf seabed in the region, respectively, and adjoining mangrove forests cover a total area of 1044 km^2. Most of its ~3700 coral reefs are located approximately 15 km to 150 km offshore. An open body of water, known as the GBR lagoon, separates the main reef matrix from the mainland and contains some 700 inshore coral reefs and islands (Hopley et al., 2007). The GBR lagoon has a water depth of around 10-20 m close to shore, and increases to 40 m towards the reef matrix, representing an area of around 238,700 km^2 (Hopley et al., 2007). Within the central part of the lagoon, water primarily moves northward and is driven by a predominant south-easterly trade wind regime from March through to October, with winds being more variable during the austral summer (Wolanski, 1994). Generally, the GBR shelf water is well mixed and the East Australian Current flows poleward and enters the shelf and outer lagoon through passages between reefs (Wolanski, 1994). The GBR region is subjected to a monsoonal climate, characterized by a wet summer (December–March), early-dry (April-July) and a late-dry (August-November) winter seasons, with between 60% and 80% of the annual rainfall occurring in the wet season (Wolanski, 1994). River floods typically last only a few days and enter the shelf as plumes mostly during the summer, with river runoff being negligible during the rest of the year. The region is characterized by tropical to subtropical water temperatures (22° to 32°C) and generally contains low dissolved nutrient concentrations relative to other coastal systems. Total dissolved inorganic nitrogen (DIN) and soluble reactive phosphate (SRP) concentrations are on the order of 0.5 and 0.1 µmol kg^{-1}, respectively and generally show little temporal and spatial variations (Lønborg et al., 2018; Lønborg et al., 2017). Particulate and organic nutrients are consistently higher than dissolved inorganic nutrients, contributing around 19% and 80% of the total nitrogen and

phosphorus concentrations, respectively (Lønborg et al., 2018; Lønborg et al., 2017). Increased nutrient concentrations and phytoplankton biomass are mainly observed in the coastal boundary zone (within the 20-m isobath) close to mangrove forests, and after large-scale weather events (e.g. storms, cyclones) that increase land runoff inshore and upwelling in the offshore areas (Alongi and McKinnon, 2005).

Sample collection – Water samples were taken during cruises carried out from September 2009 and August 2016. Samples were collected during daytime and in most instances (83% of data) from the R/V *Cape Ferguson* or R/V *Aquarius*. In order to increase the spatial coverage we included additional samples (146 samples) collected by divers on the slopes of the coral reef at water depths between 6 and 8 m (~ 1 m over the benthos).

Full-depth, continuous conductivity-temperature-depth (CTD) profiles were recorded (Seabird SBE19Plus) during each sampling event on the R/V *Cape Ferguson* or R/V *Aquarius*. The practical salinity reading from the sensor mounted on the CTD rosette frame was calibrated with water samples collected with Niskin bottles (Ocean Test Equipment**)** and analysed in the base laboratory with a salinometer (Guildline, Portasal Model 8410A). The limit of detection of this method is 0.003. For the diver-collected samples, the salinity and temperature data were derived from sensors installed on board the R/V *Cape Ferguson* (less than 50 m away from the sampling site) which are frequently calibrated as part of the Integrated Marine Observing System (IMOS: http://imos.org.au/) network. The accuracy for these measurements are ± 0.01 and ± 0.001°C for salinity and temperature respectively.

Following the CTD deployment, water samples were recovered from Niskin bottles at 2 depths (surface and 1 m over the benthos) and analysed for total alkalinity (TA), dissolved inorganic carbon (DIC), chlorophyll *a* (chl. *a*), dissolved inorganic nitrogen (Ammonium: NH_4^+ and Nitrate/Nitrite: NO_3^-/NO_2^-), soluble reactive phosphate (SRP), particulate organic carbon (POC), particulate nitrogen (PN), particulate phosphorus (PP), dissolved organic carbon (DOC), total dissolved nitrogen (TDN),

and total dissolved phosphorus (TDP). The processing and filtration of the water samples started immediately after collection. All TA and DIC samples were carefully drawn from the Niskin bottles into 250 mL bottles to avoid bubble formation and minimize headspace. In addition, divers collected TA/DIC water samples on the slopes of the coral reef. The samples were poisoned with 125 µL of saturated $HgCl_2$ to inhibit biological activity and were stored in the dark at room temperature until laboratory analyses.

Chl. *a* samples were collected by filtering between 100 and 200 mL of the sampled water through pre-combusted (450°C, 4 h) GF/F filters (pore size ~ 0.7 µm). Suspended matter (POC, PN and PP) was collected under low-vacuum on pre-combusted GF/F filters for particulate organic matter (250 mL) analysis. All filters were kept frozen (-20°C) until analysis. The samples for the dissolved phase (inorganic nutrients, DOC, TDN and TDP) analyses were immediately filtered through a 0.45 µm filter cartridge (Sartorius MiniSart) into acid-washed 10-50 mL HDPE plastic containers. Duplicate water samples for inorganic nutrients, TDN, and TDP were kept frozen (-20 ºC) until analysis. Ten mL sub-samples for DOC were collected in duplicate, preserved by adding 100 µL HCl (Scharlau 37% Ultrapure) and stored in the dark at 4°C until analysis. A detailed description of the methods used for the analysis of Chl. *a*, particulate and dissolved material can be found in the supplementary material.

Carbonate system analysis and calculations – The TA and DIC concentrations were determined from the same sample bottle using a VINDTA 3C instrument (Marianda, Germany). TA was determined by acid titration (Dickson et al., 2007) and DIC by acidification and coulometric detection (UIC 5105 Coulometer) of the evolved CO_2. Samples were not filtered, were preserved with $HgCl_2$ at the time of collection, and kept in air conditioned storage until analysis. Salinity was measured on separate samples collected from the same Niskin bottles. Analysis was performed as soon as possible after collection (within weeks), but the time period between sampling and analysis varied. Certified Reference seawater (A. G. Dickson, Scripps Institute of Oceanography, Dixon) was

analysed at the beginning, middle and end of each analytical session to confirm the quality of the measurements. Within the sample run we regularly analysed in-house seawater samples to confirm stability and allow a calculation of analytical uncertainty. There was no evidence of evaporation or $CaCO_3$ precipitation in any of the samples, but particulate matter did settle in turbid water samples. Samples were handled with extreme care so that settled particles, compacted within the lower end of the bottle, were not resuspended. Analytical samples were drawn from the middle of the bottle so settled particles were not taken up for the analyses. The VINDTA instrument was run at a controlled temperature (24°C) using a volume of 17.41 mL for the analysis of DIC, and of 98.00 mL for the analysis of TA. The standard deviation of repeated measurements was < 3 µmol kg^{-1} for TA and 5 µmol $kg^{-1}$for DIC. Using the discrete TA and DIC measurements as input parameters, we calculated other carbonate chemistry variables (pH on the total scale, and aragonite saturation state, Ω_{ar}) using the R-based package SeaCarb version 3.2 with the function "carb" (Gattuso et al., 2017), at the *in-situ* salinity and temperature. Calculations were made using the stability constant of hydrogen fluoride provided by Perez and Fraga (1987) and the carbonic acid dissociation constants determined by Lueker et al. (2000). In this study the air-sea surface flux (F) was determined from the difference between the partial pressure of CO_2 (ΔpCO_2) at the sea surface (pCO_2) and in the atmosphere (pCO_{2atm}) according to:

$$F = k_{660} \times \alpha \times \Delta pCO_2 \qquad (1)$$

where k_{660} is the gas transfer velocity or coefficient (cm h^{-1}) normalized to a Schmidt number (non-dimensional) of 660 (Wanninkhof et al., 2009), and α is the CO_2 solubility in seawater (mol^{-1} atm^{-1} m^{-3}) at *in-situ* conditions calculated from surface water temperature and salinity according to the equation Weiss (1974). A negative flux indicates a net uptake of CO_2 (sea acts as a CO_2 sink), whereas positive values represents a net CO_2 outgassing from the water body to the atmosphere. The gas transfer velocity, k_{660}, was calculated using the parameterization proposed by Ho et al. (2006). We also tested the use of other parameterizations (Liss and Merlivat, 1986; Nightingale et al., 2000a;

Nightingale et al., 2000b; Wanninkhof, 1992; Wanninkhof and McGillis, 1999). In this study, we do not discuss how the use of different gas transfer velocities could impact our results but instead refer to the previous studies which address this subject in detail (Jiang et al., 2008a; Jiang; et al., 2008b; Wanninkhof, 2014). We chose to use the monthly averaged wind speed data over the whole sampling period, as opposed to data of a higher frequency, to reduce the influence of high wind events on our flux calculations. As we used monthly averaged wind data, our air–sea CO_2 exchange estimates are conservative compared to using short term wind data which can provide higher estimates (Jiang et al., 2008b). The wind speed was acquired from the Australian Institute of Marine Science (AIMS) weather portal (http://weather.aims.gov.au/) and matched by date and location (latitude and longitude) to our carbon chemistry data. Monthly values of directly measured partial pressure of pCO_{2atm} were derived from the Cape Cleveland, Australia measuring site (Figure S1). This site is the closest, long-term source of atmospheric CO_2 data to the GBR. Its distance to some of the sampling sites (ranging between 10 and 700 km) could lead to variations in pCO_{2atm} between locations, but as the prevailing wind direction in the GBR is south easterly (from sea to land) the potential bias in pCO_{2atm} is thought to be minimal. Final calculations of pCO_2 were obtained at 1 atmospheric total pressure, with 100% saturation of water vapor and *in-situ* temperature (Weiss, 1974).

Data analysis - Salinity normalization is commonly used to correct marine carbonate system parameters (TA, DIC) for variations in salinity. In systems where river inputs are low, such as in the GBR, other processes (rain, evaporation, shelf currents, upwelling, calcification, etc.) are likely more influential on the salinity normalization step and the intercept of these relationships is therefore an unreliable indicator of the river end member concentrations. In this study, we used the method proposed by Friis et al. (2003) to calculate salinity-normalized TA (NTA) and DIC (NDIC) at SP = 35.0, which was the average salinity during the whole sampling period. This resulted in non-zero end member values of 511.6 µmol kg^{-1} for TA ($NTA_{=0}$) and 669.0 µmol kg^{-1} for DIC ($NDIC_{=0}$) (Figure 2). One out of a total of 834 data points had an abnormally low salinity (26.9), and was excluded

from the regression as it influenced the regression intercept significantly. Moreover, the contribution of calcification to annual changes in the carbonate system was examined using NTA vs NDIC plots and by superimposing our data on a nomogram. This method assumes that net primary production of one mole of organic C reduces DIC by one mole with only minor changes in TA, while calcification reduces TA by two moles and DIC by one mole for each mole of $CaCO_3$ precipitated (Ware et al., 1991). In systems where calcification dominates, there should be a linear relation between DIC and TA with a slope approaching 2.0. It was furthermore possible to account for the impact of biological activity on the TA values (TA_P) and remove the effects of organic matter formation and degradation (Fraga and Alvarez-Salgado, 2005). However, the exclusion of the effects of nutrient uptake/generation through the calculation of TA_P did not strongly alter TA values (< 2%; data not shown). This lack of effect might be linked with the very low and invariant dissolved inorganic nutrient concentrations and the heavy reliance on organic nutrients in fuelling the productivity of the GBR (Lønborg et al., 2018), which is not considered in these calculations.

In order to determine the seasonal effect of processes related ($pCO_{2,Temp}$) and those not related ($pCO_{2,Bio}$) to temperature changes on surface water pCO_2 dynamics, we used the method developed by Takahashi et al. (2002) and calculated the effect as:

$$pCO_{2,Temp} = (pCO_2)_{mean} \times \exp(0.0423 \times (T_{obs} - T_{mean})) \quad (2)$$

$$pCO_{2,Bio} = (pCO_2)_{obs} \times \exp(0.0423 \times (T_{mean} - T_{obs})) \quad (3)$$

where T is temperature (°C) and the subscripts "mean" and "obs" indicate the annual mean temperatures (T_{mean}) and the observed or measured *in-situ* temperatures (T_{obs}) (Table 1). The term $pCO_{2,Bio}$ includes the effect of multiple processes including net CO_2 utilization by primary production, net alkalinity change due to nutrient consumption and calcification, changes due to ocean freshwater balance, air-sea exchange of CO_2, and addition of CO_2 and alkalinity due to vertical mixing of subsurface waters. The term $pCO_{2,Bio}$ should therefore be seen as a "net biology" effect (Takahashi et al. 2002; Henson et al. 2018). The relative importance of each effect is expressed as the

ratio between $pCO_{2,\ Temp}$ and $pCO_{2,\ Bio}$. A ratio > 1 suggests a dominance of temperature effects over biological processes on the pCO_2 dynamics.

Regression analyses were performed using the best-fit between the two variables X and Y obtained by regression model II (Sokal and Rohlf, 1995). Prior to regressions, normality was checked and the confidence level was set at 95%, with all statistical analyses conducted in Statistica 6.0. The coefficient of variation (CV) was calculated as the (Standard deviation/Mean) × 100. Spatial distribution plots of carbonate variables were generated using the *DIVA Gridding* algorithm from the software Ocean Data View® version 4.7.10 (Schlitzer, 2016).

Results

Environmental characteristics of the Great Barrier Reef – During our study period, wind directions were predominantly equatorward with the monthly averaged wind intensities exhibiting a relatively small range between 5.0 and 9.5 m s^{-1}. Monthly mean wind speeds were slightly higher during the early and late dry seasons, which is characteristic of the trade wind regime in the GBR (Wolanski, 1994). Over the sampling period, salinity ranged from a minimum of 26.9 to a maximum of 36.2 (average ± standard deviation; 35.0 ± 0.7). The salinities were overall quite invariable and had the lowest degree of variation (CV) of all measured environmental variables (Table 1; Figure S2). Water temperature ranged between 13.2 and 31.1°C (25.7 ± 3.1°C), with the highest temperatures at low latitudes and during the wet season (Table 1; Figure S2). Chl. *a* concentration ranged between 0.01 and 2.70 µg L^{-1} (0.36 ± 0.26 µg L^{-1}), with marginally higher levels closer to shore and at mid-shelf stations during the wet season (Table 1). The DIN and SRP concentrations ranged from below the limit of detection (± 0.06 µmol kg^{-1} for DIN, and ± 0.01 µmol kg^{-1} for SRP) to 20.99 µmol kg^{-1} (0.55 ± 1.79 µmol kg^{-1}) and 1.42 µmol kg^{-1} (0.11 ± 0.14 µmol kg^{-1}), respectively (Table 1). Generally, the DIN and SRP concentrations were close to the detection limits but some elevated concentrations were found at stations closer to the shore affected by river runoff and sediment resuspension events.

The coefficients of variation (CV) demonstrated that, of the above-mentioned variables, DIN showed the largest variation followed by SRP and Chl. *a* (Table 1).

Particulate organic matter (POM) concentrations were generally slightly elevated in surface compared to bottom waters, during the wet season, and at stations closer to shore. The POC concentrations varied between 0.3 and 68.8 µmol kg^{-1} (10.3 ± 7.2 µmol kg^{-1}) (Table 1), while PN and PP ranged from 0.10 to 9.48 µmol kg^{-1} (1.4 ± 0.9 µmol kg^{-1}) and from 0.01 to 0.35 µmol kg^{-1} (0.07 ± 0.04 µmol kg^{-1}), respectively (Table 1). The CV's showed that the degree of variation was different with season but was generally highest for POC followed by PN and PP (Table 1). The average (± standard deviation) C:N:P stoichiometry of the POM pool was 186 (±182):24 (±19):1 while the median was 128:18:1, both were not significantly different from the Redfield ratio (106:16:1), suggesting a predominantly planktonic origin (Redfield et al., 1963). The large STD of our average values are due to that samples were collected in a very wide range of environments (e.g. mangrove vs. Coral Sea samples) and conditions found throughout the Great Barrier Reef. Higher levels of dissolved organic matter (DOM) were measured in surface waters during the wet season and closer to shore (Table 1), with concentrations varying between 43 and 360 µmol kg^{-1} (77 ± 20 µmol kg^{-1}) for DOC, 1.0 and 24.0 µmol kg^{-1} (6.0 ± 2.2 µmol kg^{-1}) for DON and 0.01 to 0.73 µmol kg^{-1} (0.17 ± 0.08 µmol kg^{-1}) for DOP (Table 1). The CV demonstrated that during all seasons the largest degree of variation was found for DOP, followed by DON and DOC (Table 1).

Carbonate chemistry data – In this study, we included some previously published data (Uthicke et al., 2014), but mainly unpublished data on DIC and TA collected from September 2009 to August 2016. This dataset comprises samples collected over a wide range of environmental conditions and the number of measurements varies between years and regions (Figure S3), with a total of 834 samples distributed equally between the three major seasons (wet season: 269 samples; early dry season: 273 samples; late dry season: 292 samples) (Table 2; Figure S3).

The TA values ranged between 1753 and 2409 μmol kg^{-1}, with generally higher concentrations observed during the late dry season and highest variability during the wet season (Table 2; Figure S4). In general, TA values were correlated with salinity ($R^2 = 0.74$ $p < 0.0001$; Figure 2). The salinity normalization to the average salinity (35.0) removed only a minor part (average 1 %) of the variability in TA, with the highest impact at the inshore stations during the wet season (up to 338 μmol kg^{-1}; Table 2; Figure S4). Both the TA and NTA levels did not show any apparent spatial (longitudinal or latitudinal) or temporal trends either in the annual or the seasonal datasets (Data not shown).

DIC concentrations ranged between 1549 and 2192 μmol kg^{-1}, and mean values showed highest concentrations during the late dry season and largest variability during the wet season (Table 2; Figure S5). The DIC levels were moderately correlated with salinity ($R^2 = 0.37$, $p < 0.0001$; Figure 2), and salinity normalization removed the largest (up to 261 μmol kg^{-1}) variation in the DIC data (NDIC) in the wet season (Table 2). Both the DIC and NDIC levels did not show any apparent longitudinal or latitudinal trends (Data not shown). There was no apparent long-term trend in NDIC using both annual and seasonal divided datasets over the sampling period from September 2009 to August 2016. The linear relationships between NDIC and NTA had the steepest slopes in the wet season (0.77) and flattest in the late dry season (0.44) (Figure 3). We furthermore plotted our data on diagrams by season with vectors indicating the theoretical effects of photosynthesis–respiration and calcification–dissolution (Figure S6). The slopes suggest that the importance of calcification in controlling the carbon cycle varies seasonally with a larger influence of primary production/ respiration in the wet season (Slope = 0.77), followed by the early-dry season (0.67) and then the late-dry season (0.44).

Using the measured TA and DIC, we calculated the variables pCO_2, pH and Ω_{ar}. pCO_2 reached values between 227 and 633 μatm, which were generally higher during the wet season and at stations closer to land, with surface values generally declining from north to south (Table 2; Figure 4). Linear

regression analysis showed that, over the sampling period from 2009 to 2016, the pCO_2 increased linearly ($R^2 = 0.55$, $p < 0.0001$) during the early dry season, while no long-term trends were found during the other two seasons (data not shown).

The calculated air–sea CO_2 flux varied between -6.19 and 12.17 mmol C m^{-2} d^{-1} (average ± SE: 1.44 ± 0.15 mmol C m^{-2} d^{-1}), with the maximum overall average release of CO_2 occurring in the wet season (Table S1). During the wet season, higher CO_2 fluxes were found at around 17°S and 146°E, while no clear patterns were found during the early and late dry seasons (Figure S7). Our results demonstrate that, on average, the GBR acts as a CO_2 source to the atmosphere but that spatial and seasonal variability exists (Table S1; Figure 4). The atmospheric CO_2 data used in our analysis were obtained from Cape Cleveland, Australia, showing increases over time with higher summer and lower winter values, but with lower amplitudes than at Mauna Loa (Figure S1).

The calculated $pCO_{2,\,Temp}$ to $pCO_{2,\,Bio}$ ratios showed that pCO_2 was primarily controlled by temperature (ratio = 1.28 ± 0.10) during the wet season, while temperature as well as other processes not linked with temperature changes contributed equally during the early (0.92 ± 0.20) and late dry season (0.96 ± 0.17) (Table 2).

Individual observations of pH values on the total proton scale varied between 7.69 and 8.25 (Average ± SE: 8.03 ± 0.05), with the highest variability and lowest values being observed during the wet season, and lower variability and slightly higher values in the early and late dry seasons (Table 2; Figure S8). Slightly lower pH values were found at around 17°S and 146°E during the wet season, while no clear spatial differences were found during the other seasons (Figure S9). It should also be noted that our minimum pH (7.69) would not be observed in open water environments, while previous studies in coral reef systems have demonstrated both high daily variability (up to 0.75 units) and low pH values (down to 7.59) on GBR reefs (Shaw et al., 2012).

The aragonite saturation state (Ω_{ar}) of seawater varied between 2.05 and 5.00 (3.38 ± 0.31), with slightly higher variability and values during the wet season (Table 2; Figure S8), showing that the

GBR values are supersaturated with aragonite ($\Omega_{ar} > 1$). Spatial variability in Ω_{ar} was observed at around 17°S and 146°E during the wet season, while no clear spatial differences were found during the other seasons (Figure S10).

Discussion

The GBR is a large and complex shelf system, incorporating not only the world's largest coral reef ecosystem but also multiple other ecosystems, including seagrass meadows, mangrove forests and inter-reef benthos (Hopley et al., 2007). Ocean acidification is a clear threat to the GBR and determining the temporal and spatial variability in the air-sea fluxes of CO_2 is therefore important for understanding both the biogeochemistry of the system and future impacts of ocean acidification.

Global estimates of the coastal ocean CO_2 uptake and release currently contain large uncertainties (Regnier et al., 2013). Previous work in both temperate and tropical coastal waters have shown that CO_2 fluxes can vary pronouncedly both spatially and temporally (e.g. Dinauer and Mucci , 2017; Chen et al., 2013; Gattuso et al., 1996; Ware et al., 1991). For the tropical coastal waters of the GBR, there is a paucity of data, with earlier reports on the air-sea CO_2 fluxes suggesting that the system acts as a net source (Suzuki et al., 2001) but also a net sink (Shaw and McNeil, 2014). As these studies involved either short-term sampling efforts (Kawahata et al., 2000; Suzuki and Kawahata, 2003; Suzuki et al., 2001) or work on individual coral reefs (Albright et al., 2013; Cyronak et al., 2014; Shaw and McNeil, 2014; Shaw et al., 2015), their extrapolation to the whole GBR, given their limited temporal and spatial coverage is questionable. In our calculations of the CO_2 flux, we used monthly averaged wind and pressure data, which are considered more representative for the GBR, so we do not include the effect of short-term variability in the wind speed on the air–sea CO_2 exchange. The use of monthly averaged wind speeds entails that our calculated air–sea CO_2 exchange estimates are conservative, and using short-term wind data would have likely provided approximately 20% higher estimates (Jiang et al. 2008b). Our results, in accordance with previous studies, are largely

independent of the gas transfer coefficient and algorithms used (Table S1). Our calculations show that despite spatial-temporal variabilities , the GBR is, in all seasons, overall a net source of CO_2 to the atmosphere, which is consistent with the current paradigm for tropical coastal waters (Bauer et al., 2013; Cai et al., 2006; Jahnke, 2010).

The possible reasons why the GBR serves as a source of CO_2 could be related to multiple factors, with previous studies in low-latitude coastal waters suggesting that these include: (1) elevated metabolic rates of heterotrophic organisms due to external inputs of organic material, combined with enhanced water temperatures, (2) production, storage and dissolution of $CaCO_3$, (3) inorganic and organic carbon inputs from mangroves, and rivers, and/or (4) warming of offshore waters flowing onto the shelf with subsequent outgassing of pCO_2.

The GBR is an oligotrophic coastal system with generally low nutrient levels (Table 1) and productivity compared to temperate systems. Previous studies in the GBR have determined pelagic metabolic rates (production and respiration) using oxygen consumption and production measurements in bottles, demonstrating that the pelagic system is overall net autotrophic (production to respiration ratio > 1) and therefore the pelagic component should act as a sink for atmospheric CO_2 (McKinnon et al., 2017; McKinnon et al., 2013). The GBR is generally shallow and light often reaches the seafloor. Part of the primary production therefore takes place in the benthic environment (corals, seagrass, micro-phytobenthos and macro-algae), but the extent and importance of benthic production and respiration is currently unknown. The importance of net community production and calcification on changes in coral reef carbonate chemistry using the slope of TA-DIC nongrams has recently been reviewed (Cyronak et al., 2018). Our observed slopes (0.77- wet season, 0.67- early-dry season and 0.44- late-dry season) are comparable to those found by Cyronak et al. (2018), and they suggested that, for the GBR, net community production accounted for 80 ± 5% of the variations in the slopes. This is consistent with results of recent studies showing that coral reefs can modify the carbonate chemistry of overlying waters (e.g Albright et al., 2013; Shaw et al. 2012). As corals are

abundant on the shelf, it is likely that they, as well as mangroves, seagrasses, plankton, and benthos, through their productivity and respiratory processes, alter water chemistry on the shelf. However, due to the extreme complexity of the GBR and our current poor understanding of the physical transport, water circulation within the system and biogeochemical cycles, it is currently not possible to confidently conclude which of these are the most important contributors.

The production, storage and dissolution of $CaCO_3$ form important components of the carbon cycle in the GBR. $CaCO_3$ is primarily produced by benthic corals and calcifying algae, and the sediment burial rates are generally high (30– 260 mol C m^{-2} yr^{-1}) on mid and outer shelf coral reef platforms, representing the largest carbon reservoir in those areas (Brunskill et al., 2002). Storage and dissolution of $CaCO_3$ in reef sediments has been suggested as key determinants on how coral reef ecosystems will be impacted by ocean acidification (Eyre et al., 2014; Eyre et al., 2018). Regrettably, with our current dataset, we are not able to estimate the impact of $CaCO_3$ storage and dissolution on the air-sea CO_2 flux, while some impact will be evident, a large-scale influence seems unlikely, as reef platforms represent less than 13% of the GBR shelf area.

Mangroves and rivers export large amounts of both inorganic and organic material to tropical coastal waters (Alongi and McKinnon, 2005; Sippo et al., 2016). Whilst mangroves occupy only around 0.5% of the total global ocean area, they transfer disproportionate large amounts of TA and DIC to coastal environments, which combined with elevated heterotrophic microbial activity due to the export and degradation (respiration) of labile organic matter, can enhance sea to air CO_2 exchange (Alongi et al., 2013; Borges, 2003). Previous studies in the GBR have shown that the impact of mangrove derived organic material can be large locally, being normally confined to an area less than 20 km from the mangroves (Alongi and McKinnon, 2005). Tropical rivers export ~45 Tmol C yr^{-1} of carbon (both inorganic and organic) to the coastal ocean globally (Huang et al., 2012), corresponding to a disproportional large fraction of the global river inputs (30% of PIC, 60% of DIC and 62% of DOC;(Dai et al., 2012; Huang et al., 2012). River waters in the tropics are therefore

generally supersaturated in CO_2 and have high DOC concentrations. When entering the coastal ocean, the excess CO_2 carried by these rivers is outgassed while DOC is partly degraded further adding to the CO_2 source (Lønborg and Álvarez-Salgado, 2012). Generally, the GBR is rapidly flushed by Coral Sea water. For comparison, an equivalent volume of water delivered to the southern GBR by rivers within one year is flushed through the GBR from the Coral Sea within an 8 hour period (Choukroun et al., 2010). Although the rivers jointly discharge on average 17 km^3 of freshwater annually into the GBR and are suggested to alter the ecology of the inshore GBR, these floods are relatively short-lived and hence the carbonate chemistry of the GBR as a whole is generally not river-dominated. Salinities ~ 2.5 km from the mouths of seven major rivers averaged 34.0 ± 2.0 (range 25.0 to 36.0; measured continuously over a two-year period; Lønborg et al. unpubl. data) and are also only marginally lower than those found in the Coral Sea (~35.5). Shelf evaporation and rainfall has previously been shown to modify the salinity especially in nearshore areas of the GBR. The impact of evaporation is especially evident during the dry season when evaporation exceeds the freshwater input from rainfall and rivers, and in some instances even creating "hypersaline" waters (~36-37) (Andutta et al., 2011; Wang et al., 2007). Rainfall is more pronounced in the summer wet season, but the volume, timing and duration of precipitation events varies largely between years depending on several factors, e.g. the number and paths of tropical cyclones. Therefore, if samples were collected after a period of strong evaporation or rainfall, salinity changes and the corresponding variation in the relationship with the carbonate system variables would be influenced by dilution or distillation (Robbins, 2001). Currently, both evaporation and rainfall rates are poorly constrained for the GBR shelf, so quantification of the impact is not possible. A global analysis also suggested that the river end-member concentration can only be reliably derived from the y-intercept of the linear relationships between TA and DIC with salinity in river-dominated systems (e.g. estuaries) (Jiang et al. 2014). Away from freshwater input, other processes (evaporation, upwelling, calcification, etc.) may be more important, and the intercept can be

decoupled from the river end member concentration. Thus, since the coastal waters of the GBR 1) has multiple river end-members, 2) is impacted by many physical and biological processes, 3) salinity is sensitive to precipitation, evaporation and freshwater input from sources other than rivers (i.e. groundwater) and 4) both TA and DIC levels showed no clear cross shelf trend, suggests that the salinity normalisation step used in this study does not provide robust estimates of the riverine impact in the GBR. Therefore, most likely cross shelf input of Coral Sea water as well as the contribution from precipitation, evaporation, rivers and benthic processes determine the resulting salinity and carbon variable relationships. Previous studies have similarly shown that indicators of terrestrial organic matter are limited to sediments less than 10 km from the river mouth with most indicators being linked with mangroves sources (Currie and Johns, 1989; Susic and Alongi, 1997), suggesting that both rivers and mangroves are likely to influence the CO_2 air-sea flux locally but not over large spatial scales.

Mixing of colder open ocean with warmer shelf water has combined with evaporation been shown to increase the pCO_2 in tropical waters, resulting in supersaturation relative to the atmosphere and a net CO_2 release (Chen et al., 2013; Takahashi et al., 2002). Therefore, cross-shelf advection of Coral Sea surface water onto the shallow GBR shelf and progressive evaporation would lead to a supersaturation of the system with respect to atmospheric pCO_2 and cause an outgassing to the atmosphere (Chen et al., 2006a; Chen et al., 2006b; Chen et al., 2013; Takahashi et al., 2002). In our analysis, we separated the effects of temperature-independent and temperature-dependent processes, showing that surface water pCO_2 levels during the wet season were primarily temperature controlled (T/B ratio = 1.28 ± 0.10), while temperature and temperature independent processes contributed equally during the early (0.92 ± 0.20) and late dry seasons (0.96 ± 0.17). These findings suggest that, in the GBR, temperature dependent physical and biogeochemical processes are partly controlling the pCO_2 and the air-sea flux.

In our dataset, slightly lower pH and Ω_{ar} were only found at around 17°S and 146°E during the wet season, while no evident latitudinal or longitudinal trends were found during the other seasons. This suggests that reefs in the GBR are spatially (both across the shelf and with latitude) subjected to differences in water acidity (pH) and saturation state for coral reef formation (Ω_{ar}). Further research and monitoring effort are therefore needed to determine how the GBR will react to predicted changes in the carbonate system and acidification.

Conclusion

The data described in this study quantifies for the first time the large scale seasonal and spatial air-sea CO_2 fluxes in the Great Barrier Reef. Our analysis shows that there exists spatial and temporal variability in this flux but that overall the Great Barrier Reef is a net source of CO_2 to the atmosphere. These fluxes are likely being controlled by cross-shelf advection of oversaturated Coral Sea surface water into the system and enhanced water temperatures combined with progressive evaporation, which leads to CO_2 oversaturation relative to the atmosphere and a net release. Therefore, increases in atmospheric and water column CO_2, and seawater temperature will likely have a larger impact on the status of the GBR as a CO_2 source than future potential decreases in coral abundance and their metabolic influence on seawater CO_2 chemistry.

Acknowledgments

Financial support for this study was provided by the by the Great Barrier Reef Foundation's "Resilient Coral Reefs Successfully Adapting to Climate Change" programme in collaboration with the Australian Government, and the Australian Institute of Marine Science. The authors thank John Pfitzner for his huge efforts in organizing the sample collection and analysis. We thank the crew of the R/V *Cape Ferguson* and R/V *Aquarius* for help at sea and Irena Zagorskis and Johnstone Davidson for their help in collecting water samples. Irena Zagorskis is thanked for making the maps

included in the manuscript. We also thank Michele Skuza for her huge effort in helping to obtain the dataset. The field chlorophyll *a* and nutrient data included in the manuscript were obtained with support from the Great Barrier Reef Marine Park Authority, through funding from the Australian Government Reef Program and from the Australian Institute of Marine Science. Data from the R/V Cape Ferguson's underway system were sourced from the Integrated Marine Observing System (IMOS) - IMOS is a national collaborative research infrastructure, supported by the Australian Government. The R/V Cape Ferguson's underway data are provided by the Australian Ocean Data Network (AODN) Portal (https://portal.aodn.org.au/) and the AIMS Data Catalogue (http://www.aims.gov.au/docs/data/data.html).We thank the associated editor and three anonymous reviewers for their detailed comments and useful suggestions that helped improve the manuscript.

Table 1. Biological, chemical and physical properties of water samples at the time of collection. The minimum (Min), maximum (Max), amplitude (maximum minus minimum level), average values (± standard deviation), coefficient of variance (CV), and number of samples (N) for salinity (Sal.), temperature (Temp.), chlorophyll *a* (Chl. *a*), dissolved inorganic nitrogen (DIN= NH_4^++ NO_3^-/NO_2^-) and soluble reactive phosphate (SRP), dissolved organic carbon (DOC), nitrogen (DON) and phosphorus (DOP), particulate organic carbon (POC), nitrogen (PN) and phosphorus (PP) are shown for the wet, early dry and late dry seasons and for the whole year

Season		Sal.	Temp. °C	Chl. *a* µg l-1	DIN µmol kg^{-1}	SRP µmol kg^{-1}	DOC µmol kg^{-1}	DON µmol kg^{-1}
Wet	Min	26.9	25.8	0.10	0.01	0.00	61	1.5
	Max	36.2	31.1	2.70	1.75	0.24	360	10.0
	Amplitude	9.3	5.3	2.59	1.75	0.24	299	8.5
	Avg. (± STD)	34.7 (± 1.0)	28.5 (± 1.1)	0.48 (± 0.31)	0.24 (± 0.33)	0.07 (± 0.05)	84 (± 27)	5.6 (± 1.7)
	CV	3	4	65	135	68	33	30
	N	265	233	181	180	179	173	127
Early dry	Min	31.9	15.7	0.00	0.00	0.00	52	3.4
	Max	35.8	28.9	1.31	11.41	0.92	160	24.0
	Amplitude	3.8	13.2	1.31	11.41	0.92	109	20.6
	Avg. (± STD)	34.9 (± 0.6)	24.1 (± 2.6)	0.34 (± 0.20)	0.52 (± 1.75)	0.11 (± 0.13)	78 (± 16)	6.4 (± 2.3)
	CV	2	11	59	337	117	20	37
	N	248	217	229	226	225	214	171

Late dry	Min	34.4	13.2	0.00	0.01	0.01	43	1.0
	Max	36.1	30.3	1.90	20.99	1.42	143	19.1
	Amplitude	1.7	17.1	1.90	20.98	1.41	100	18.1
	Avg. (± STD)	35.4 (± 0.2)	24.5 (± 2.8)	0.30 (± 0.24)	0.67 (± 2.29)	0.13 (± 0.17)	71 (± 14)	5.9 (± 2.2)
	CV	1	11	82	341	132	19	37
	N	291	257	278	280	279	268	230
All year	Min	26.9	13.2	0.01	0.00	0.00	43	1.0
	Max	36.2	31.1	2.70	20.99	1.42	360	24.0
	Amplitude	9.3	17.9	2.69	20.99	1.42	317	23.0
	Avg. (± STD)	35.0 (± 0.7)	25.7 (± 3.04)	0.36 (± 0.26)	0.51 (± 1.79)	0.11 (± 0.14)	77 (± 20)	6.0 (± 2.2)
	CV	2	12	73	350	129	26	36
	N	804	707	688	686	683	655	528

Table 2. A summary of the carbon chemistry of water samples collected in the Great Barrier Reef. The minimum (Min), maximum (Max), amplitude (maximum minus minimum level), average values (± standard deviation), coefficient of variance (CV) for Total Alkalinity (TA), Dissolved Inorganic Carbon (DIC), salinity normalized TA and DIC (NTA , NDIC), together with surface partial pressure of carbon dioxide (pCO_2), and effect of biological processes ($pCO_{2,Bio}$) and temperature ($pCO_{2,\ Temp}$) on pCO_2 dynamics, pH and Aragonite saturation state (Ω_{ar}) are shown for the wet, early dry and late dry seasons and for the whole year. N- number of TA and DIC samples measured.

Season		TA µmol kg^{-1}	NTA µmol kg^{-1}	DIC µmol kg^{-1}	NDIC µmol kg^{-1}	pCO_2 µatm	$pCO_{2,\ Bio}$ µatm
Wet	Min	1753	2125	1549	1812	305	248
	Max	2409	2443	2192	2194	633	536
	Amplitude	656	318	643	382	328	288
	Avg. (± STD)	2271 (± 58)	2284 (± 31)	1972 (± 55)	1982 (± 41)	430 (± 47)	386 (± 39)
	CV	3	1	3	2	11	10
	N	269		269			
Early dry	Min	2101	2222	1847	1925	332	321
	Max	2343	2365	2122	2110	531	602
	Amplitude	242	143	275	185	198	281
	Avg. (± STD)	2279 (± 37)	2286 (± 17)	1984 (± 37)	1989 (± 31)	387 (± 38)	400 (± 43)
	CV	2	1	2	2	10	11
	N	273		273			
Late dry	Min	2273	2263	1925	1916	227	293
	Max	2376	2330	2132	2125	572	621
	Amplitude	103	67	207	209	346	328
	Avg. (± STD)	2312 (± 15)	2293 (± 11)	2011 (± 33)	1996 (± 31)	397 (± 42)	405 (± 43)
	CV	1	0	2	2	11	11
	N	292		292			
All year	Min	1753	2125	1549	1812	227	250
	Max	2409	2443	2192	2194	633	627
	Amplitude	656	318	643	382	406	377
	Avg. (± STD)	2288 (± 44)	2288 (± 22)	1989 (± 45)	1989 (± 35)	404 (± 46)	401 (± 43)
	CV	2	1	2	2	11	11
	N	834		834			

References

Albright, R., Langdon, C. and Anthony, K.R.N., 2013. Dynamics of seawater carbonate chemistry, production, and calcification of a coral reef flat, central Great Barrier Reef. Biogeosciences, 10(10): 6747-6758.

Alongi, D., Bouillon, S., Duarte, C.M., Ramanathan, A. and Robertson, A., 2013. Carbon and nutrient fluxes across tropical river-coastal boundaries in the Anthropocene, Biogeochemical Dynamics at Major River-Coastal Interfaces: Linkages with Global Change. Cambridge University Press, pp. 373-396.

Alongi, D.M. and McKinnon, A.D., 2005. The cycling and fate of terrestrially-derived sediments and nutrients in the coastal zone of the Great Barrier Reef shelf. Mar Pollut Bull, 51(1-4): 239-52.

Andersson, A.J., Mackenzie, F.T. and Lerman, A., 2005. Coastal ocean and carbonate systems in the high CO_2 world of the Anthropocene. American Journal of Science, 305: 875–918.

Andutta, F.P., Ridd, P.V. and Wolanski, E., 2011. Dynamics of hypersaline coastal waters in the Great Barrier Reef. Estuarine, Coastal and Shelf Science, 94(4): 299-305.

Ashley, D. and Alfonoso, M., 2017. Spatial variability in surface-water pCO2 and gas exchange in the world's largest semi-enclosed estuarine system: St. Lawrence Estuary (Canada). Biogeosciences, 14: 3221–3237.

Balch, W.M., 2005. Calcium carbonate measurements in the surface global ocean based on Moderate-Resolution Imaging Spectroradiometer data. Journal of Geophysical Research, 110(C7).

Bauer, J.E. et al., 2013. The changing carbon cycle of the coastal ocean. Nature, 504(7478): 61-70.

Borges, A.V., 2003. Atmospheric CO_2 flux from mangrove surrounding waters. Geophysical Research Letters, 30(11).

Borges, A.V. and Abril, G., 2012. Carbon Dioxide and Methane Dynamics in Estuaries. In: E. Wolanski and D.S. McLusky (Editors), Treatise on Estuarine and Coastal Science Academic Press, 2012, pp. 119-161.

Borges, A.V. et al., 2004. Variability of the Gas Transfer Velocity of CO_2 in a Macrotidal Estuary (the Scheldt). Estuaries, 27: 593–603.

Brunskill, G.J., 2010. An overview of tropical margins. In: K.-K. Liu, Atkinson, L., Quinones, R., Talaue-McManus, L. (Editor), Carbon and Nutrient fluxes in Continental Margins: a Global Synthesis. Springer, Berlin, pp. 423–426.

Brunskill, G.J., Zagorskis, I. and Pfitzner, J., 2002. Carbon Burial Rates in Sediments and a Carbon Mass Balance for the Herbert River Region of the Great Barrier Reef Continental Shelf, North Queensland, Australia. Estuarine, Coastal and Shelf Science, 54(4): 677-700.

Cai, W.-J., Dai, M. and Wang, Y., 2006. Air-sea exchange of carbon dioxide in ocean margins: A province-based synthesis. Geophysical Research Letters, 33(12).

Cai, W.J., 2011. Estuarine and coastal ocean carbon paradox: CO_2 sinks or sites of terrestrial carbon incineration? Ann Rev Mar Sci, 3: 123-45.

Chen, C.-T.A. and Borges, A.V., 2009. Reconciling opposing views on carbon cycling in the coastal ocean: Continental shelves as sinks and near-shore ecosystems as sources of atmospheric CO_2. Deep Sea Research Part II: Topical Studies in Oceanography, 56(8-10): 578-590.

Chen, C.-T.A., Hou, W.-P., Gamo, T. and Wang, S.L., 2006a. Carbonate-related parameters of subsurface waters in the West Philippine, South China and Sulu Seas. Marine Chemistry, 99(1-4): 151-161.

Chen, C.-T.A., Wang, S.-L., Chou, W.-C. and Sheu, D.D., 2006b. Carbonate chemistry and projected future changes in pH and $CaCO_3$ saturation state of the South China Sea. Marine Chemistry, 101(3-4): 277-305.

Chen, C.T.A. et al., 2013. Air–sea exchanges of CO_2 in the world's coastal seas. Biogeosciences, 10(10): 6509-6544.

Choukroun, S., Ridd, P.V., Brinkman, R. and McKinna, L.I.W., 2010. On the surface circulation in the western Coral Sea and residence times in the Great Barrier Reef. Journal of Geophysical Research, 115(C6): C06013.

Currie, B.R. and Johns, R.B., 1989. An organic geochemical analysis of terrestrial biomarkers in a transect of the Great Barrier Reef lagoon. Australian Journal of Marine and Freshwater Research, 40: 275–284.

Cyronak, T. et al., 2018. Taking the metabolic pulse of the world's coral reefs. PLoS One, 13: e0190872.

Cyronak, T., Schulz, K.G., Santos, I.R. and Eyre, B.D., 2014. Enhanced acidification of global coral reefs driven by regional biogeochemical feedbacks. Geophysical Research Letters, 41(15): 5538-5546.

Dai, M., Yin, Z., Meng, F., Liu, Q. and Cai, W.-J., 2012. Spatial distribution of riverine DOC inputs to the ocean: an updated global synthesis. Current Opinion in Environmental Sustainability, 4(2): 170-178.

Dickson, A.G., Sabine, C.L. and Christian, J.R., 2007. Guide to best practices for ocean CO_2 measurements. PICES special publication, 3.

Doney, S.C., Fabry, V.J., Feely, R.A. and Kleypas, J.A., 2009. Ocean acidification: the other CO_2 problem. Annual Review of Marine Science, 1: 169-92.

Eyre, B.D., Andersson, A.J. and Cyronak, T., 2014. Benthic coral reef calcium carbonate dissolution in an acidifying ocean. Nature Climate Change, 4: 969-976.

Eyre, B.D. et al., 2018. Coral reefs will transition to net dissolving before end of century. Science, 359: 908–911.

Fraga, F. and Alvarez-Salgado, X.A., 2005. On the variation of alkalinity during phytoplankton photosynthesis. Ciencias marinas, 31: 627-639.

Gattuso, J.P. et al., 2017. Seacarb: seawater carbonate chemistry with R. R package version 3.2, The Comprehensive R Archive Network.

Gattuso, J.P., Frankignoulle, M. and Wollast, R., 1998. Carbon and carbonate metabolism in coastal aquatic ecosystems Annual Review of Ecology and Systematics, 29: 405–434.

Gattuso, J.P., Pichon, M., Delesalle, B., Canon, C. and Frankignoulle, M., 1996. Carbon fluxes in coral reefs. I. Lagrangian measurement of community metabolism and resulting air-sea CO_2 disequilibrium. Marine Ecology Progress Series: 109-121.

Henson, S. A., Humphreys, M.P., Land, P. E., Shutler, J. D., Goddijn-Murphy, L., and Warren, M., 2018. Controls on open-ocean North Atlantic Δ*p*CO2 at seasonal and interannual time scales are different. Geophysical Research Letters, 45. https://doi.org/10.1029/2018GL078797

Ho, D.T. et al., 2006. Measurements of air-sea gas exchange at high wind speeds in the Southern Ocean: implications for global parameterization. Geophysical research letters, 31: L16611

Hopley, D., Smithers, S.G. and Parnell, K., 2007 The Geomorphology of the Great Barrier Reef: Development, Diversity and Change, . Cambridge Univ. Press, Cambridge, UK.

Huang, T.-H., Fu, Y.-H., Pan, P.-Y. and Chen, C.-T.A., 2012. Fluvial carbon fluxes in tropical rivers. Current Opinion in Environmental Sustainability, 4(2): 162-169.

Jahnke, R.A., 2010. Global synthesis. In: K.-K. Liu, L. Atkinson, R. Quinones and L. Talaue-McManus (Editors), Carbon and Nutrient Fluxes in Continental Margin. Springer, Berlin, Germany, pp. 597-615.

Jiang, L.-Q., Cai, W.-J., Wanninkhof, R., Wang, Y. and Luger, H., 2008a. Air-sea CO2 fluxes on the U.S. South Atlantic Bight: Spatial and seasonal variability. Journal of Geophysical Research, 113: C07019.

Jiang, L.-Q., Cai, W.-J. and Wang, Y., 2008b. A comparative study of carbon dioxide degassing in river- and marine-dominated estuaries. Limnology and oceanography, 53: 2603-2615.

Kawahata, H., Suzuki, A., Ayukai, T. and Goto, K., 2000. Distribution of the fugacity of carbon dioxide in the surface seawater of the Great Barrier Reef. Marine Chemistry, 72(2): 257-272.

Kinsey, D.W. and Hopley, D., 1991. The significance of coral reefs as global carbon sinks—response to greenhouse. Global and Planetary Change, 3: 363-377.

Le Quéré, C. et al., 2016. Global Carbon Budget 2016. Earth System Science Data, 8(2): 605-649.

Lenton, A., Tilbrook, B., Matear, R., Sasse, T.P. and Nojiri, Y., 2016. Historical reconstruction of ocean acidification in the Australian region. Biogeosciences, 13: 1753-1765.

Liss, P.S. and Merlivat, L., 1986. Air-sea gas exchange rates: Introduction and synthesis. In: Buat-M´enard (Editor), The Role of Air-Sea Exchange in Geochemical Cycling. D. Reidel Publishing Company Boston, Massachusetts, USA, pp. 113–127.

Lønborg, C. and Álvarez-Salgado, X.A., 2012. Recycling versus export of bioavailable dissolved organic matter in the coastal ocean and efficiency of the continental shelf pump. Global biogeochemical cycles 26: GB3018.

Lønborg, C., Álvarez-Salgado, X.A., Duggan, S. and Carreira, C., 2018. Organic matter bioavailability in tropical coastal waters: The Great Barrier Reef. Limnology and Oceanography, 63: 1015-1035.

Lønborg, C. et al., 2017. Seasonal organic matter dynamics in the Great Barrier Reef lagoon: contribution of carbohydrates and proteins. Continental Shelf Research, 38: 95–105.

Lueker, T.J., Dickson, A.G. and Keeling, C.D., 2000. Ocean pCO2 calculated from dissolved inorganic carbon, alkalinity, and equations for K1 and K2: validation based on laboratory measurements of CO2 in gas and seawater at equilibrium. Marine Chemistry, 70: 105-119.

Maher, D.T., Santos, I.R., Golsby-Smith, L., Gleeson, J. and Eyre, B.D., 2013. Groundwater-derived dissolved inorganic and organic carbon exports from a mangrove tidal creek: The missing mangrove carbon sink? Limnology and oceanography, 58: 475-488.

McKinnon, A.D., Duggan, S., Logan, M. and Lønborg, C., 2017. Plankton Respiration, Production, and Trophic State in Tropical Coastal and Shelf Waters Adjacent to Northern Australia. Frontiers in Marine Science, 4.

McKinnon, A.D., Logan, M., Castine, S.A. and Duggan, S., 2013. Pelagic metabolism in the waters of the Great Barrier Reef. Limnology and Oceanography, 58(4): 1227-1242.

Milliman, J.D., 1993. Production and accumulation of calcium carbonate in the ocean—budget of a nonsteady state. Global biogeochemical cycles, 7: 927–957.

Mongin, M. et al., 2016. The exposure of the Great Barrier Reef to ocean acidification. Nat Commun, 7: 10732..

Nightingale, P.D., Liss, P.S. and Schlosser, P., 2000a. Measurements of air-sea gas transfer during an open ocean algal bloom. Geophysical Research Letters, 27(14): 2117-2120.

Nightingale, P.D. et al., 2000b. In situ evaluation of air-sea gas exchange parameterizations using novel conservative and volatile tracers. Global Biogeochemical Cycles, 14(1): 373-387.

Nittrouer, C.A., Brunskill, G.J. and Figueiredo, A.G., 1995. Importance of tropical coastal environments. Geo-Marine Letters, 15: 121-126.

Perez, F.F. and Fraga, F., 1987. Association constant of fluoride and hydrogen ions in seawater. Marine Chemistry, 21: 161-168.

Redfield, A.C., Ketchum, B.K. and Richards, F.A., 1963. The influence of organisms on the composition of sea-water. In: M.N. Hill (Editor), The sea, vol. 2, The composition of sea water: Comparative and descriptive oceanography. Wiley-Interscience, pp. 26- 77.

Regnier, P. et al., 2013. Anthropogenic perturbation of the carbon fluxes from land to ocean. Nature Geoscience, 6(8): 597-607.

Robbins, P.E., 2001. Oceanic carbon transport carried by freshwater divergence- Are salinity normalizations useful? Journal of Geophysical Research, 106: 30,939-30,946,.

Shaw, E.C. and McNeil, B.I., 2014. Seasonal variability in carbonate chemistry and air–sea CO_2 fluxes in the southern Great Barrier Reef. Marine Chemistry, 158: 49-58.

Shaw, E.C., McNeil, B.I. and Tilbrook, B., 2012. Impacts of ocean acidification in naturally variable coral reef flat ecosystems. Journal of Geophysical Research, 117: C03038.

Shaw, E.C., Phinn, S.R., Tilbrook, B. and Steven, A., 2015. Natural in situ relationships suggest coral reef calcium carbonate production will decline with ocean acidification. Limnology and Oceanography, 60(3): 777-788.

Sippo, J.Z., Maher, D.T., Tait, D.R., Holloway, C. and Santos, I.R., 2016. Are mangroves drivers or buffers of coastal acidification? Insights from alkalinity and dissolved inorganic carbon export estimates across a latitudinal transect. Global Biogeochemical Cycles, 30(5): 753-766.

Smith, S.V. and Key, G.S., 1975. Carbon dioxide and metabolism in marine environments. . Limnology and oceanography, 20: 493-495.

Smith, S.V. and Pesret, F., 1974. Processes of carbon dioxide flux in the Fanning Island lagoon. Pacific Science, 28: 225-245.

Sokal, F.F. and Rohlf, F.J., 1995. Biometry. Freeman, New York.

Susic, M. and Alongi, D.M., 1997. Determination of terrestrial markers in marine environments by gas chromatography-mass-selective detection compared to high-performance liquid chromatography-fluorescence detection. Journal of Chromatography A, 758: 243–254.

Suzuki, A. and Kawahata, H., 1999. Partial pressure of carbon dioxide in coral reef lagoon waters: comparative study of atolls and barrier reefs in the Indo-Pacific Oceans. Journal of oceanography, 55: 731-745.

Suzuki, A. and Kawahata, H., 2003. Carbon budget of coral reef systems: an overview of observations in fringing reefs, barrier reefs and atolls in the Indo-Pacific region. Tellus, 55B: 428-444.

Suzuki, A., Kawahata, H., Ayukai, T. and Goto, K., 2001. The oceanic CO2 system and carbon budget in the Great Barrier Reef, Australia. Geophysical Research Letters, 28(7): 1243-1246.

Takahashi, T., Olafsson, J., Goddard, J.G., Chipman, D.W. and Sutherland, S.C., 1993. Seasonal variation of CO_2 and nutrients in the high-latitude surface oceans: A comparative study. Global Biogeochemical Cycles, 7(4): 843-878.

Takahashi, T. et al., 2002. Global sea–air pCO_2 flux based on climatological surface ocean pCO_2, and seasonal biological and temperature effects. Deep Sea Research Part II: Topical Studies in Oceanography, 49(9): 1601-1622.

Thomas, H., Bozec, Y., Ellkaly, K. and Baar, H.J.W., 2004. Enhanced Open Ocean Storage of CO_2 from Shelf Sea Pumping. Science, 304: 1005-1008.

Tsunogai, S., Watanabe, S. and Sato, T., 1999. Is there a "continetal shelf pump" for the absorption of atmospheric CO_2? Tellus, 518: 701-712.

Uthicke, S., Furnas, M. and Lønborg, C., 2014. Coral reefs on the edge? Carbon chemistry on inshore reefs of the great barrier reef. PLoS One, 9(10): e109092.

Wang, Y., Ridd, P.V., Heron, M.L., Stieglitz, T.C. and Orpin, A.R., 2007. Flushing time of solutes and pollutants in the central Great Barrier Reef lagoon, Australia. Marine and Freshwater Research, 58(8): 778.

Wanninkhof, R., 1992. Relationship between wind-speed and gasexchange over the ocean. Journal of Geophysical Research, 97: 7373– 7382.

Wanninkhof, R., 2014. Relationship between wind speed and gas exchange over the ocean revisited. Limnology and oceanography methods, 12: 351-362.

Wanninkhof, R., Asher, W.E., Ho, D.T., Sweeney, C. and McGillis, W.R., 2009. Advances in quantifying air-sea gas exchange and environmental forcing. Ann Rev Mar Sci, 1: 213-44.

Wanninkhof, R. and McGillis, W.R., 1999. A cubic relationship between air–sea CO_2 exchange and wind speed. Geophysical Research Letters, 26: 1889–1892.

Ware, J.R., Smith, S.V. and Reaka-Kudla, M.L., 1991. Coral reefs: sources or sinks of atmospheric CO_2? Coral Reefs, 11: 127-130.

Weiss, R.F., 1974. Carbon dioxide in water and seawater: The solubility of a non-ideal gas. Marine Chemistry, 2: 203–215.

Wolanski, E., 1994. Physical Oceanographic Processes of the Great Barrier Reef. CRC Press, Boca Raton.

Figure legends

Figure 1. Map showing the Great Barrier Reef where samples (coloured dots) were collected during the wet (December–March), early dry (April-July) and late dry (August-November) seasons from September 2009 to August 2016. The arrows indicate the main ocean currents: South Equatorial Current (SEC), East Australian current (EAC) and the Gulf of Papua current (GPC), which enter the shelf and outer lagoon through passages between reefs. The arrow close to shore indicates the coastal current which is predominantly equatorward.

Figure 2. Plots of the linear relationship between: (a) salinity and total alkalinity (TA) and (b) salinity and dissolved inorganic carbon (DIC). Solid lines represent the corresponding regression and error bars are standard errors. R^2 = coefficient of determination, p = significance level. The encircled point was omitted from the regression analysis.

Figure 3. Relationships between salinity normalized dissolved inorganic carbon (NDIC) and total alkalinity (NTA) for the (a) wet (December-March), (b) early dry (April-July) and (c) late dry (August-November) seasons. The regression lines and corresponding equations were obtained using model II linear regression and error bars are standard errors. R^2 = coefficient of determination, p = significance level.

Figure 4. Surface distribution of (a), (b), (c) water carbon dioxide (pCO_2) concentrations and (d), (e), (f) the calculated air-sea flux of CO_2 ($F\ CO_2$) during the wet (December-March; (a), (d)), early dry (April-July; (b), (e)) and late dry (August-November; (c), (f)) seasons. The colour scales for each row of graphics is given to the right. Images created using Ocean Data View (Schlitzer, 2015).

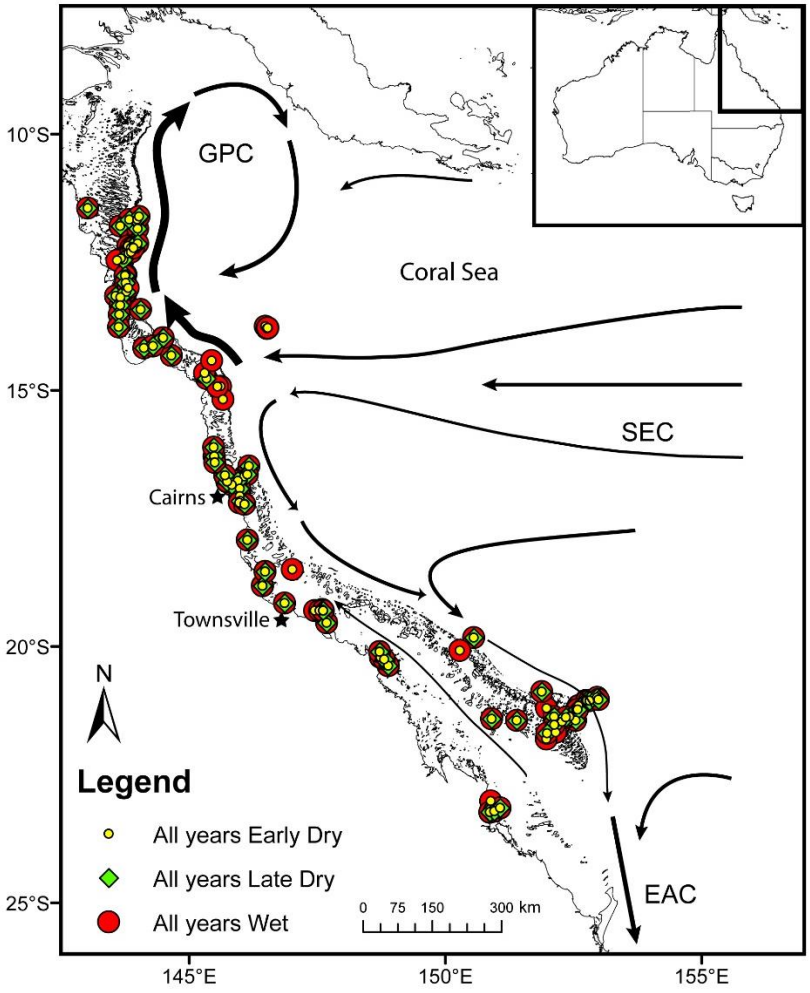

Figure 1.

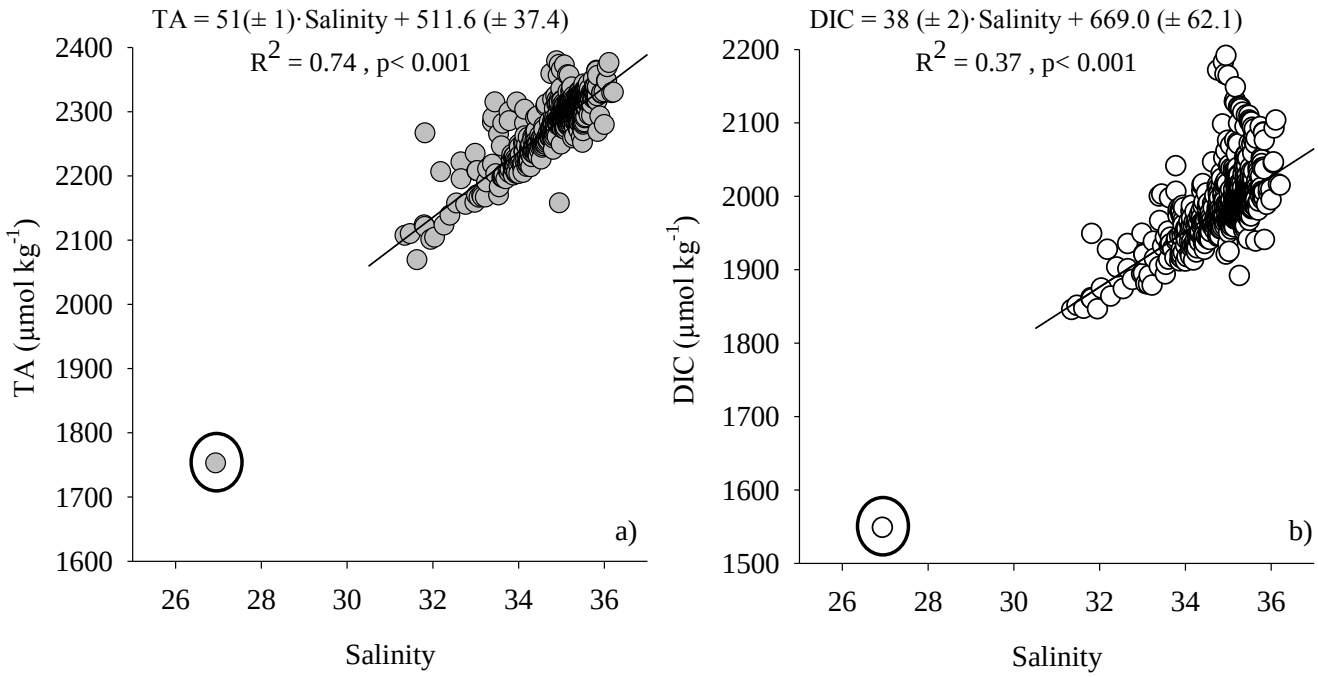

Figure 2.

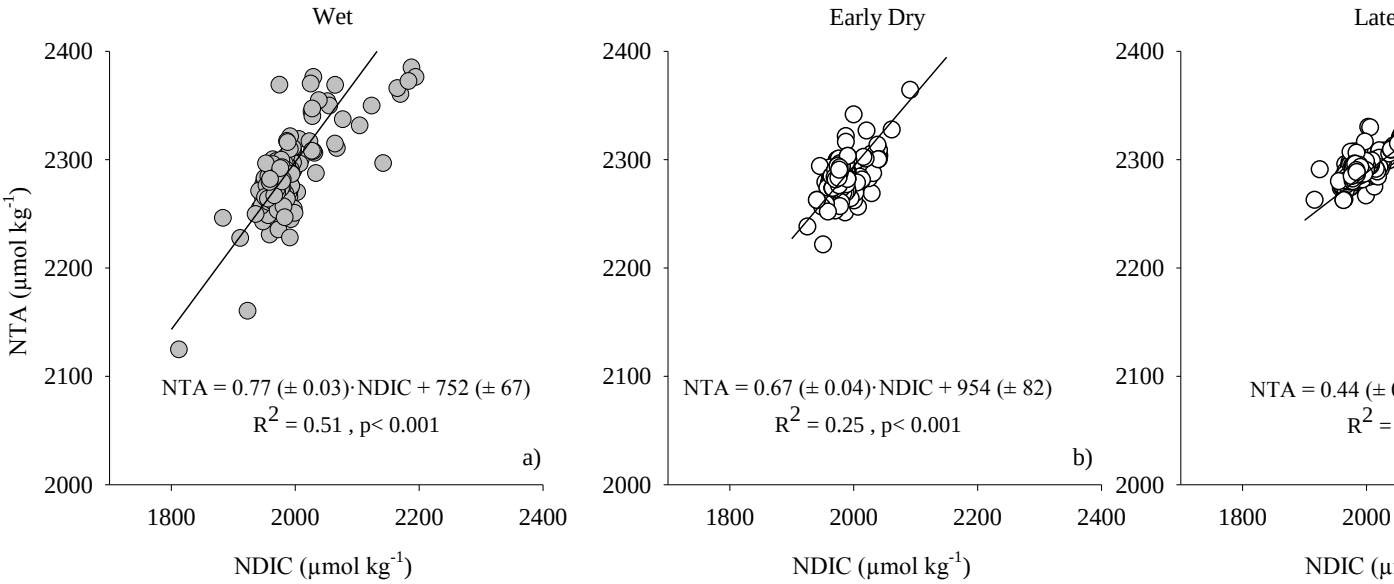

Figure 3.

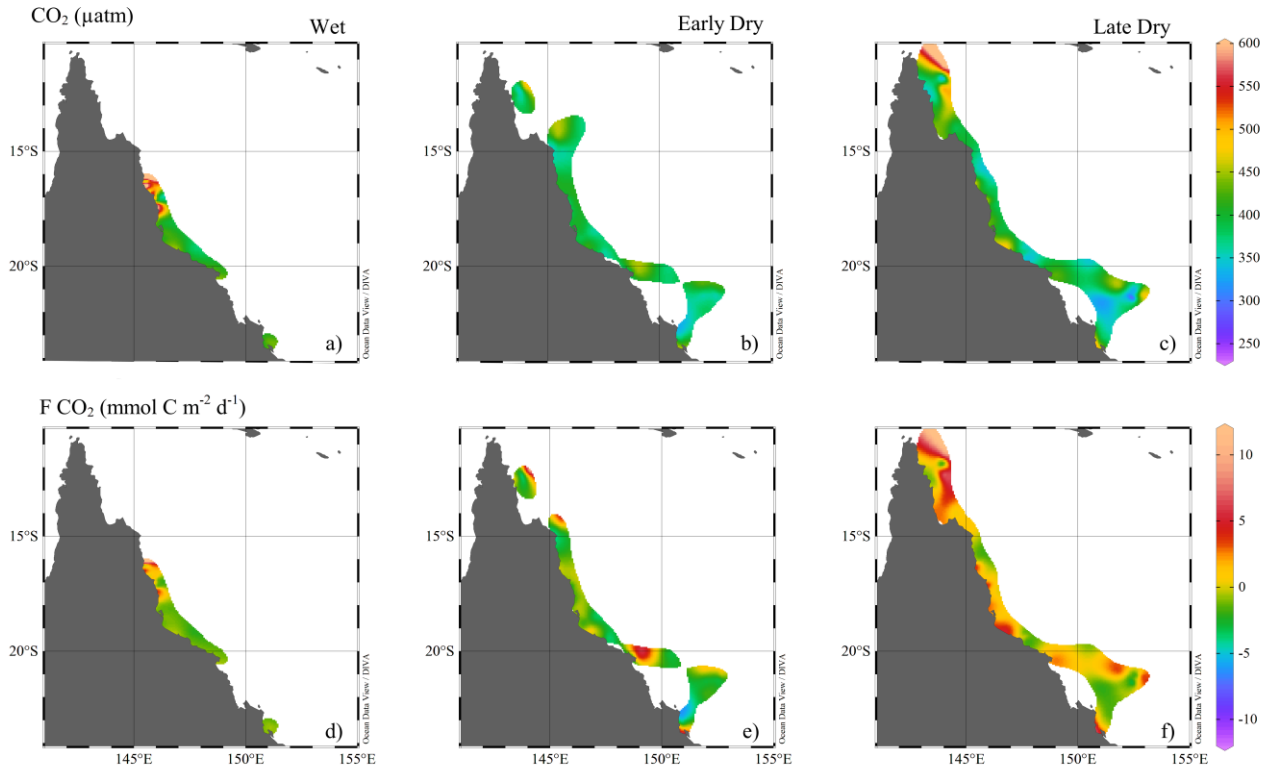

Figure 4.

Highlights:

- Seasonal variations in air-sea CO_2 fluxes on the Great Barrier Reef reveal a strong CO_2 release during the early-dry season
- The Great Barrier Reef is overall a net source of CO_2.
- CO_2 fluxes are largely controlled by cross-shelf advection of oversaturated warm surface waters from the Coral Sea

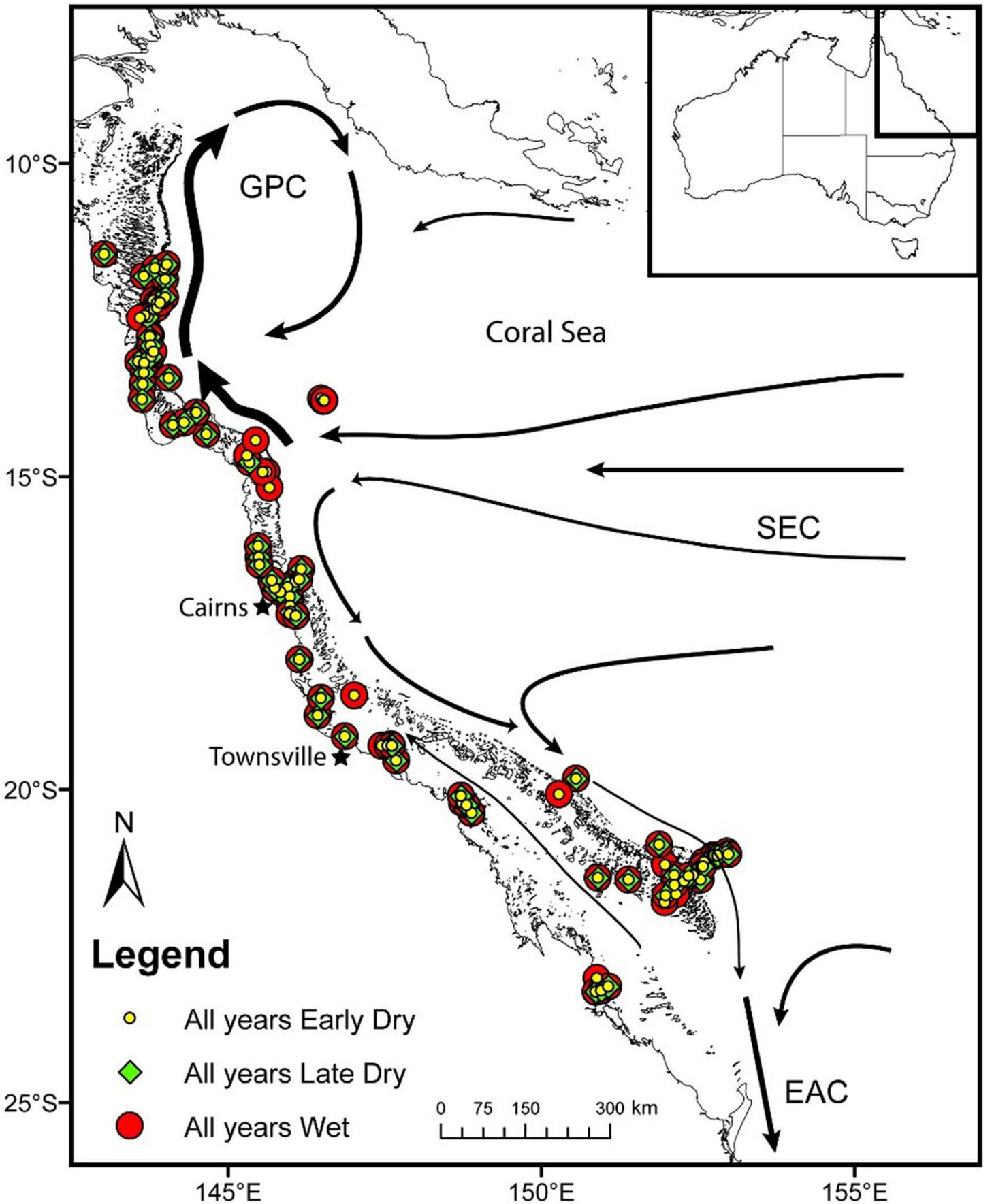
GPC
Coral Sea
SEC
Cairns
Townsville
EAC
10°S
15°S
20°S
25°S
145°E
150°E
155°E
N
Legend
All years Early Dry
All years Late Dry
All years Wet
0 75 150 300 km

Figure 1

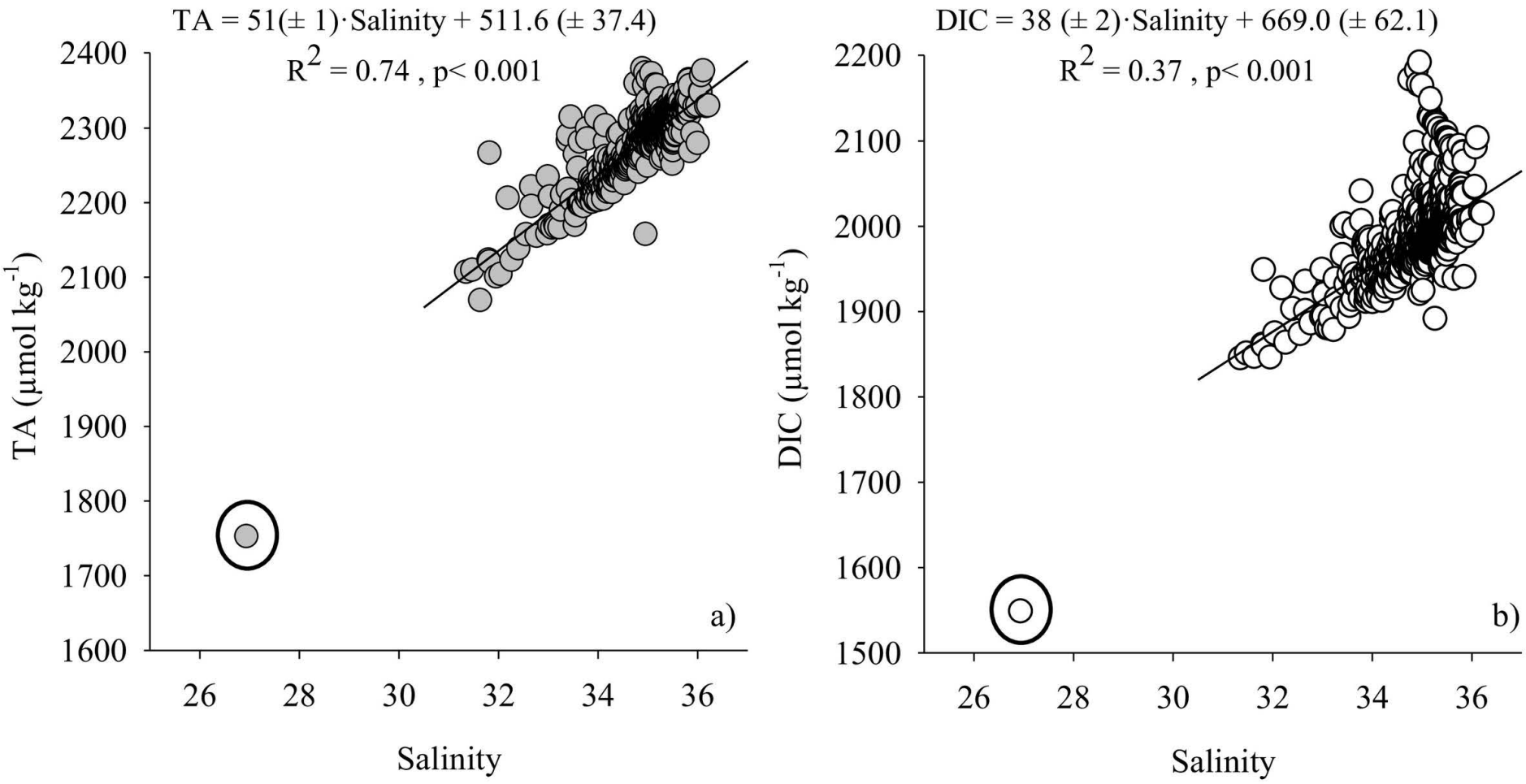
TA = 51(± 1)·Salinity + 511.6 (± 37.4)
R2 = 0.74 , p< 0.001
TA (µmol kg-1)
2400
2300
2200
2100
2000
1900
1800
1700
1600
26
28
30
32
34
36
Salinity
a)
DIC = 38 (± 2)·Salinity + 669.0 (± 62.1)
R2 = 0.37 , p< 0.001
DIC (µmol kg-1)
2200
2100
2000
1900
1800
1700
1600
1500
26
28
30
32
34
36
Salinity
b)

Figure 2

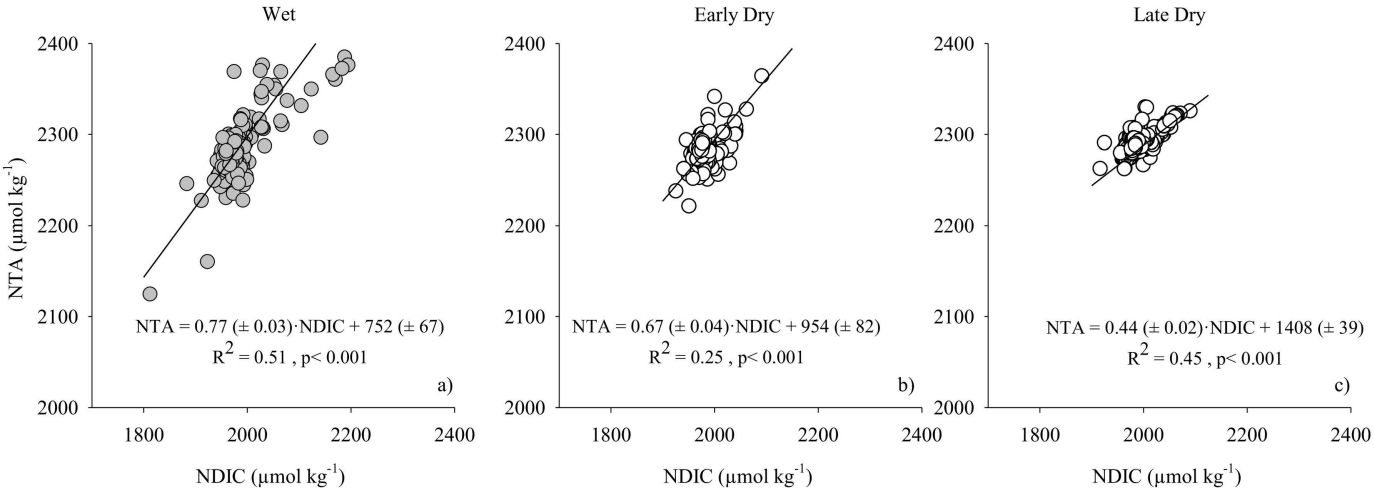
Wet
Early Dry
Late Dry
NTA (µmol kg-1)
NDIC (µmol kg-1)
2400
2300
2200
2100
2000
1800
2000
2200
2400
NTA = 0.77 (± 0.03)·NDIC + 752 (± 67)
R2 = 0.51 , p< 0.001
a)
NTA = 0.67 (± 0.04)·NDIC + 954 (± 82)
R2 = 0.25 , p< 0.001
b)
NTA = 0.44 (± 0.02)·NDIC + 1408 (± 39)
R2 = 0.45 , p< 0.001
c)

Figure 3

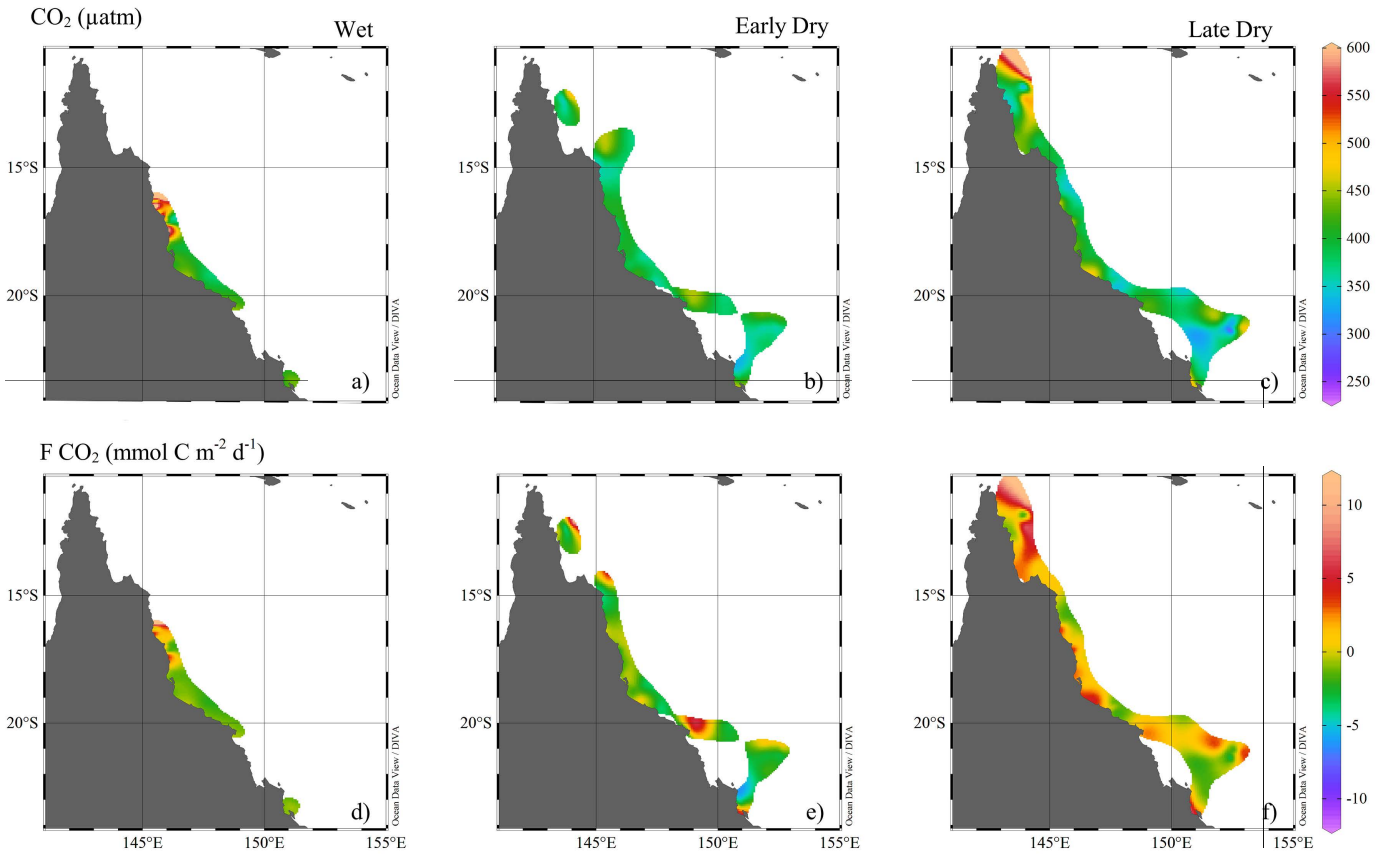

Figure 4